Georgia Journal of Science

Volume 78 *No. 2 Scholarly Contributions from the Membership and Others*

Article 10

2020

Demonstration of a Distributed Bragg Reflector for Polyvinylcarbazole and Cadmium Sulfide Layers: Modeling and Comparison to Experimental Results

Javier E. Hasbun
jhasbun@westga.edu

L. Ajith DeSilva
University of West Georgia, ldesilva@westga.edu

Demonstration of a Distributed Bragg Reflector for Polyvinylcarbazole and Cadmium Sulfide Layers: Modeling and Comparison to Experimental Results

Acknowledgements

The authors would like to thank the University of West Georgia Institutional STEM Excellence program for their financial support for this research. We also acknowledge Jared Thacker who started a simulation for a two-period DBR system as an undergraduate research project while at UWG.

DEMONSTRATION OF A DISTRIBUTED BRAGG REFLECTOR FOR POLYVINYLCARBAZOLE AND CADMIUM SULFIDE LAYERS: MODELING AND COMPARISON TO EXPERIMENTAL RESULTS

Javier E. Hasbun and L. Ajith DeSilva*
Department of Physics, University of West Georgia,
1601 Maple St., Carrollton, Georgia, 30118
*corresponding author: ldesilva@westga.edu

ABSTRACT

Light wave propagation in a periodically stratified medium has many applications in physics, mathematics, and engineering. The subject is of interest to students, teachers, and researchers, as it presents a great opportunity to focus on principles of optics and to understand the basics of mathematical modeling. A complete theory of wave propagation can be derived using Born's optics theory. We employed that theory to determine the reflectivity of a one-dimensional distributed Bragg reflector (DBR) and do simulations using MATLAB. A DBR is a photonic crystal consisting of alternating layers of materials with different refractive indices. In this study, we modeled theoretical reflectivity of a four-period DBR and compared with experimental results previously constructed on a glass substrate and reported by DeSilva et al. (2018). Each period consists of a layer of polyvinyl carbazole and a layer of cadmium sulfide. We used the Cauchy equation for the simulation of the wavelength dependency of the cadmium sulfide refractive index in a wavelength range between 400 and 1000 nm. The theory obtained a center wavelength and a reflectivity for each of the DBR periods in good agreement with the experimental results. Finally, in the appendix, we include a simple MATLAB script that demonstrates the application of the theory to a DBR.

Keywords: distributed Bragg reflectors, photonic structures, Cauchy equation, characteristic matrix.

INTRODUCTION

Light propagation aspects in a dielectric medium including photonic crystals have been studied extensively over the past decades (Tkeshelashvili 2013; Joannopoulos et al. 2008; Cavalcanti et al. 2006; Khreis and Elhassan 2013; Duta et al. 2016). This is due to the interesting physics dielectric media possess and their potential applications (Jewell at al. 1991; John 1987; Leem at al. 2014; Soman and Anthony 2018; Zeng et al. 2008). One such device is called a *distributed Bragg reflector* (DBR). DBRs are made of multiple layers of alternating refractive index materials in a periodic array. Each period consists of two different refractive index materials with each layer having a thickness equivalent to a quarter of the optical wavelength (Schubert et al. 2007). When light waves propagate in such periodic structures, each boundary causes partial reflection while the rest of the light is refracted. As the periodicity increases, more light tends to reflect and, for a particular wavelength range, it is possible for the device to become a

high-quality reflector. The basics of thin film interference are generally used to explain that a quality reflector is formed by the combination of many such reflections. This happens when each optical layer thickness or path length is equal to one fourth of the light wavelength. In a DBR, a stopband occurs for reflected wavelengths in whose range no light can be transmitted (Joannopoulos et al. 2008) and, in these situations, the device behaves essentially as though it were a mirror; that is, for certain wavelengths. Both the reflectivity and the stopband width can be increased by increasing the number of periods as well as by increasing the refractive index difference of the alternating layers in a period (Joannopoulos et al. 2008). In designing these structures, the device's properties can be manipulated to suit specific applications (Cavalcanti et al. 2006; Leem at al. 2014; Jewell at al. 1991; Soman and Anthony 2018; Zeng et al. 2008).

DBRs are the fundamental constituents in many optoelectronic devices, including resonance cavity light emitting diodes that enable photon quantization; these, in turn, lead to control spontaneous emission (Jewell at al. 1991; Noda et al. 2007) and directionality resulting in vertical cavity surface lasers (Hirose et al. 2014). Vertical cavity surface lasers have the advantage over standard edge-emitting lasers because of their increased power and efficiency (Hirose et al. 2014; Yu at al. 2018). The literature; for example, Khreis and Elhassan (2013), John (1987), Leem at al. (2014), and Zeng et al. (2008); abounds with of descriptions of many other devices whose applications take advantage of photonic crystals.

Successful fabrication of such devices requires careful designing through mathematical modeling and computer simulations. In our present work, a theoretical foundation is found in *Principles of Optics* (Born and Wolf 1999), which we employed to determine the reflectivity of a one-dimensional distributed Bragg reflector. Further, we show a comparison between the theory and the data obtained from an organic/inorganic hybrid four-period DBR system, which we fabricated previously (DeSilva 2018). In this paper we show how the theory makes use of the so-called *characteristic matrix* in obtaining the theoretical reflectivity for a one-dimensional DBR structure. Other important properties that the theory allows us to calculate are the center wavelength of the DBR's stopband and the reflectivity maximum at that wavelength. For the purposes of the interested reader, in the appendix, a simple MATLAB (2020) program is included which conveys the application of the mathematical modeling and which can be used for pedagogical as well as for research purposes.

EXPERIMENTAL

The DBR dealt with in this paper consists of alternating layers of poly(9-vinylcarbazole) (PVK - organic) and cadmium sulfide (CdS - inorganic) materials. The experimental detail of the construction of the DBR follows our previous work (DeSilva 2018). The device was fabricated by spin coating (EDC-650-15B, Laurell Technologies Corporation) alternating layers of PVK and CdS layers. A 0.2 M solution of thiourea and a 0.1 M solution of cadmium nitrate, both dissolved in water via sonication, were combined and spin coated at 2,000 RPM upon a glass microscope slide (Fisher Scientific). Each sample was then heated for 5 min at a temperature of 120^{o}C to form a nominal thickness of 65 nm CdS film. Next a solution consisting of 0.5 g of PVK dissolved in 20.0 g of chlorobenzene was applied to the top of the CdS film and spin coated at 1,000 RPM to obtain a nominal thickness of 90 nm PVK film. The sample was then heated again at 120^{o}C for 5 min to allow all of the solvent to evaporate resulting in a single period of the

CdS/PVK layers. This procedure was repeated for each period of alternating PVK and CdS layers. All chemicals used had a purity of 99% or above and were purchased from Fisher Scientific. This paper focuses on Bragg reflectors of 1–4 periods so this process was repeated as needed.

After the DBR was made, it was placed on an optical table where an experimental setup (Ocean Optics) for data recording was located. A tungsten halogen light source (HL 2000, Ocean Optics) was shined directly at the DBR (the light being normal to the interface of the first material) using a 400 μm premium grade reflection probe and then the data were analyzed from a UV Vis USB4000 spectrometer.

THEORY

It is of much importance for teachers and students alike to acquire an understanding of the theoretical application of the concepts mentioned in the introduction, the details of which we briefly outline for clarity and pedagogical reasons. The theory considers an arbitrary linearly polarized electromagnetic wave propagating in the z-direction towards a DBR at an angle of incidence θ_1 (Born and Wolf 1999). In the special case of linear polarization, the electromagnetic wave can be broken down into transverse electric, magnetic wave field components and, without loss of generality, the y-z plane is taken to be the plane of incidence, as shown in Figure 1.

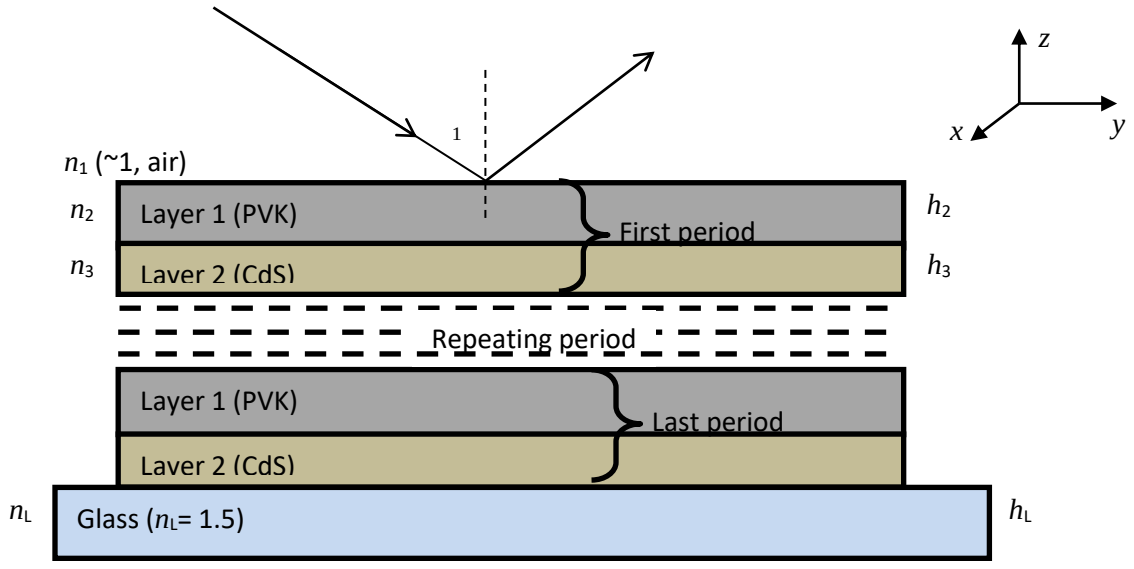

Figure 1. A sketch of a DBR which is a periodic system of alternating layers of two different refractive index materials (n_2 and n_3) with layer thicknesses of h_2, h_3. The light initially incident from a medium with refractive index of n_1, which is normally air. The substrate has a refractive index of n_L of thickness of h_L, and θ_1 is the initial angle of incidence.

We assume that field components of waves propagating in the *y*-direction are represented by equations (1–6) (Joannopoulos et al. 2008; Born and Wolf 1999).

$$E_x = U(z)e^{i(k_0\alpha y-\omega t)}, \quad (1)$$

$$H_y = V(z)e^{i(k_0\alpha y-\omega t)}, \quad (2)$$

$$H_z = W(z)e^{i(k_0\alpha y-\omega t)}, \quad (3)$$

$$H_x = U(z)e^{i(k_0\alpha y-\omega t)}, \quad (4)$$

$$E_y = -V(z)e^{i(k_0\alpha y-\omega t)}, \quad (5)$$

$$E_z = -W(z)e^{i(k_0\alpha y-\omega t)}, \quad (6)$$

Equations 1–3 and 4–6 correspond to transverse electric and transverse magnetic waves respectively (Joannopoulos et al. 2008; Khreis and Elhassan 2013; Born and Wolf 1999). The quantities *U(z), V(z)*, and *W(z)* are referred to as the amplitude functions (Khreis and Elhassan 2013; Born and Wolf 1999), which are related to one another through three equations. Two of these equations are coupled first order linear ordinary differential equations and the other equation is an equality stating the proportionality of *V* and *W* and, for this reason, any information about *W* can be deduced from *V*. Since the amplitude functions are related to one another, and they are factors in the fields for both transverse waves, then the amplitude functions relate the fields of the two waves together.

The amplitude functions can be organized in a 2× 2 square matrix, the characteristic matrix, and which is referred to as simply *the matrix* for the remainder of this paper. Maxwell's equations employ boundary conditions such that *U* and *V* are known at the plane *z* = 0. The facts about the matrix are as follows:

(1) since the amplitude functions depend on *z*, the matrix is a function of *z*;
(2) the matrix elements are the particular solutions of the differential equations involving *U, V*;
(3) because *U* and *V* are functions of *z*, the characteristic matrix itself relates the fields of the transverse waves from the plane *z* = 0 to any other *z*-plane that is specified, thus fully describing the propagation of light in the DBR.

In the case of a DBR consisting of two material layers, we have two matrices,

$$M_2 = \begin{bmatrix} \cos\beta_2 & -\frac{i}{p_2}\sin\beta_2 \\ -ip_2\sin\beta_2 & \cos\beta_2 \end{bmatrix}, \quad (7)$$

$$M_3 = \begin{bmatrix} \cos\beta_3 & -\frac{i}{p_3}\sin\beta_3 \\ -ip_3\sin\beta_3 & \cos\beta_3 \end{bmatrix}. \quad (8)$$

These matrices represent the characteristic matrices of the two material layers that make up the DBR, where $\beta_q = \frac{2\pi}{\lambda_0} n_q h_q \cos\theta_q$, $p_q = n_q \cos\theta_q$, with $q = 2,3,\cdots$, λ_0 is the reduced wavelength, n_q is the refractive index of the specified material, h_q is the

thickness of the material, and θ_q is the angle that the incident/transmitted wave makes with the axis of stratification (z-axis). In order to get the matrix for one period, we simply multiply the two matrices associated with the two layers and obtain the matrix

$$M_{2,2} = \begin{bmatrix} m_{11} & m_{12} \\ m_{21} & m_{22} \end{bmatrix} = \begin{bmatrix} \cos\beta_2 \cos\beta_3 - \frac{p_3}{p_2}\sin\beta_2 \sin\beta_3 & -i\left(\frac{1}{p_3}\cos\beta_2 \sin\beta_3 + \frac{1}{p_2}\sin\beta_2 \cos\beta_3\right) \\ -i\left(p_2 \sin\beta_2 \cos\beta_3 + p_3 \cos\beta_2 \sin\beta_3\right) & \cos\beta_2 \cos\beta_3 - \frac{p_2}{p_3}\sin\beta_2 \sin\beta_3 \end{bmatrix}. \quad (9)$$

In our work it is not enough to have the matrix for one period. The matrix for N periods is desired for experimental comparison purposes as regards more DBR periods. This is accomplished by raising equation (9) to the N^{th} power which requires more computational time than using the alternate procedure illustrated by Born and Wolf (1999); that is, matrix theory allows a simple yet effective modification to the matrix elements of the matrix for one period. In order to get the matrix for N periods the matrix elements for one period are multiplied by a combination of Chebyshev polynomials, δ_i for i = 1,2... N; for example, $\delta_0(x)$ =1, $\delta_1(x)$ = 2x, $\delta_2(x)$ = 4x^2-1, $\delta_3(x)$ = 8x^3-4x, etc, obtained by $\delta_i(x) = \sin\left[(i+1)\cos^{-1}x\right]/\sqrt{1-x^2}$.

The final matrix for N periods is shown below, along with the matrix elements definitions.

$$M_{2,N} = \begin{bmatrix} M_{11,N} & M_{12,N} \\ M_{21,N} & M_{22,N} \end{bmatrix}, \quad (10)$$

$$M_{11,N} = \left(\cos\beta_2 \cos\beta_3 - \frac{p_3}{p_2}\sin\beta_2 \sin\beta_3\right)\delta_{N-1}(a) - \delta_{N-2}(a), \quad (11)$$

$$M_{12,N} = -i\left(\frac{1}{p_3}\cos\beta_2 \sin\beta_3 + \frac{1}{p_2}\sin\beta_2 \cos\beta_3\right)\delta_{N-1}(a), \quad (12)$$

$$M_{21,N} = -i\left(p_2 \sin\beta_2 \cos\beta_3 + p_3 \cos\beta_2 \sin\beta_3\right)\delta_{N-1}(a), \quad (13)$$

$$M_{22,N} = \left(\cos\beta_2 \cos\beta_3 - \frac{p_2}{p_3}\sin\beta_2 \sin\beta_3\right)\delta_{N-1}(a) - \delta_{N-2}(a), \quad (14)$$

where

$$a = \cos\beta_2 \cos\beta_3 - \frac{1}{2}\left(\frac{p_2}{p_3} + \frac{p_3}{p_2}\right)\sin\beta_2 \sin\beta_3. \quad (15)$$

Our goal was to calculate the theoretical reflectance at each wavelength of the electromagnetic spectrum. The reflection coefficient can be put in terms of the matrix elements of N periods. The reflection coefficient is given by

$$r_N = \frac{\left(M_{11,N} + M_{12,N}p_L\right)p_1 - \left(M_{21,N} + M_{22,N}p_L\right)}{\left(M_{11,N} + M_{12,N}p_L\right)p_1 + \left(M_{21,N} + M_{22,N}p_L\right)}, \quad (16)$$

where

$$p_1 = n_1\cos\theta_1, \quad p_L = n_L\cos\theta_L, \quad (17)$$

and the reflectance is obtained from

$$R_N = |r_N|^2, \tag{18}$$

with θ_1 as the initial incident angle (~0) and $\theta_L = n_L\sqrt{1-\left(n_1 \sin\theta_1 / n_L\right)^2}$ as the final exit angle. The appendix contains a simple version of a MATLAB (2020) script that demonstrates the application of the above theory to a DBR.

RESULTS

The physical system studied in this paper deals with four periods**.** In Figure 2 we show a specific example of a structure with two periods. The reason that the thicknesses (h_2, h_3) and the refractive index of cadmium sulfide (n_3) are left unknown is that there was not a viable way of measuring the thicknesses of the material layers nor was the refractive index of CdS initially known. Thus, h_2, h_3 were obtained through theoretically fitting the experimental data (Table I). The refractive index of CdS varies significantly in the region of the electromagnetic spectrum range studied; for this reason, a CdS-specific Cauchy equation is required. Cauchy's equation is an empirical relationship between the refractive index and the wavelength (Schubert et al. 2007). The Cauchy equation for CdS, as employed here, is

$$n_3 = A + \frac{B}{\lambda^2} - \frac{C}{\lambda^4} - Die^{-E(1-F/\lambda)}. \tag{19}$$

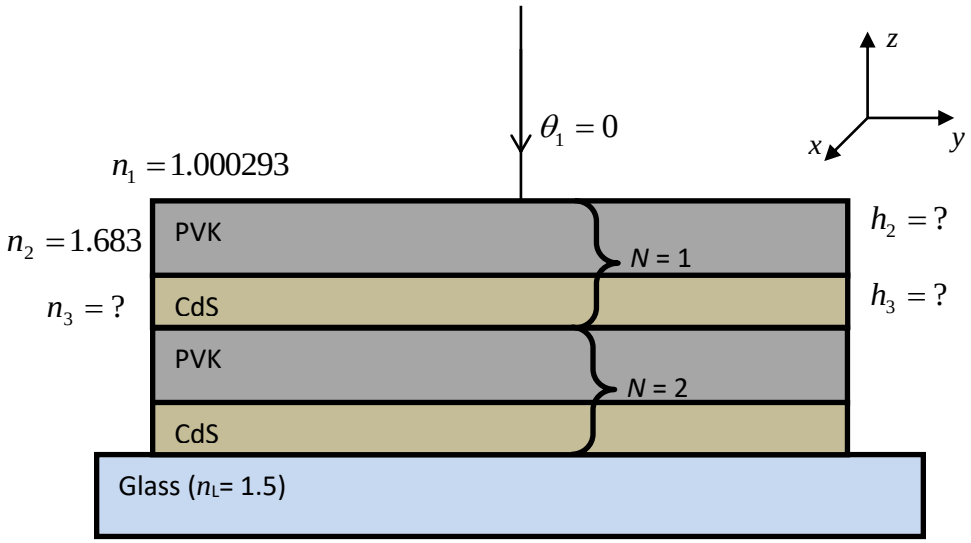

Figure 2. A sketch of a 2-period DBR example (N = 2) of a system similar to the one considered in our study. Both layer thicknesses and the refractive index of CdS, (h_3 and n_3) are experimentally unknown; also, while the PVK refractive index (n_2) is known its layer thickness (h_2) is left unknown. The unknowns are found by theoretical modeling through data best fitting.

Table I shows the parameters used in the Cauchy equation and which were found to give the best theoretical fits to the data of Figure 3. The table includes the layer widths indicated in Figure 2, corresponding to the PVK and the CdS layers, respectively. Also included in this table are the values of the center wavelength (λ_{max}) at which the maximum value of the reflectance occurs and whose value is R_{max}.

Table I. The parameters obtained for the various periods (N) of our DBR system. The parameters A, B, C, D, E, and F are those of the Cauchy equation (19), while h_2 and h_3 are associated with the PVK and the CdS layers' widths, respectively, for each of the periods, N. The value of λ_{max} and R_{max} are the center wavelength at which maximum reflectance occurs, respectively, in the theoretical plots of Figure 3.

N	h_2(nm)	h_3(nm)	A	B(nm^2) x10^4	C(nm^4) x10^4	D	E	F(nm)	λ_{max}(nm)	R_{max}
1	50	47.437	2.19	1.93	-1.93	-0.1810	-0.00147	-0.00880	673	0.273
2	50	65.063	2.4	1.93	-1.93	-0.0486	0.00248	-0.00859	606	0.510
3	50	59.395	3.08	1.93	-1.93	0.1500	0.00924	-0.00987	621	0.643
4	92.037	80.530	1.67	1.93	-1.93	-0.1610	0.00669	0.00597	614	0.783

In Figure 3 we show the theoretical curves obtained using equations (18) and (19), compared to experimental.

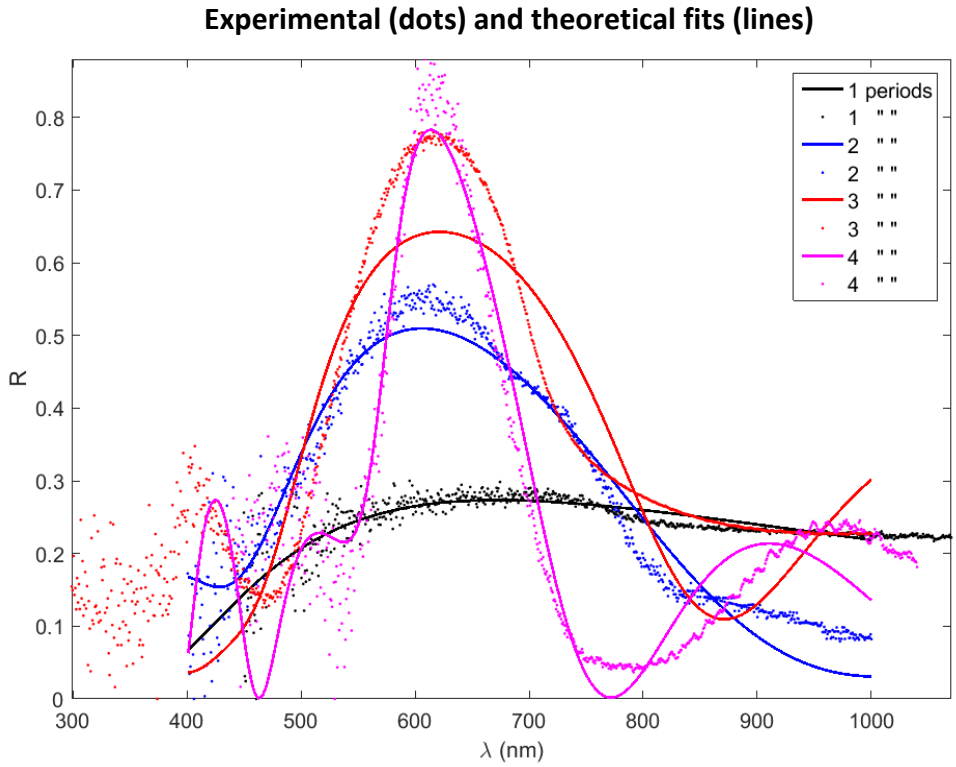

Figure 3. The plot of reflectivity versus wavelength using the Cauchy equation and the fit parameters based on equation (19) and the reflectivity R in equation (18). Experimental data are represented by dots while the solid line is the simulation in which the Cauchy equation is also incorporated to fit the parameters of equation (19).

The solid curves are the best fits that could be obtained from the theoretical calculations with the parameters shown in Table I, which also includes the two thicknesses of the PVK and CdS layers (h_2, h_3,) mentioned earlier in Figure 2, corresponding to each of our N = 1,2,3 and 4 period structures.

CONCLUSIONS

In this paper, light reflectance in a DBR consisting of various periods of alternating layers of PVK and CdS has been studied. When white light from a tungsten-halogen source was directed normally to the DBR, reflectance maxima from approximately 28%, 51%, 64%, and 80% for primary wavelengths of 673, 606, 621, and 614 nm, for periods 1, 2, 3, and 4, respectively, were obtained. This means that a DBR consisting of these materials will always reflect this primary wavelength. As can be seen from the experiments, the reflectance can be increased by increasing the number of periods of the Bragg Reflector. The theoretical calculations are consistent with the experimental findings. In the appendix we include a simple version of a MATLAB (2020) script that applies the theory to a DBR. For those readers interested in extending this work, a further point of research could be performing experiments and theoretical calculations with the goal of finding out how many periods are needed to gain as much as 99% reflectance for a primary wavelength. This question plays a role in the quest for better and higher efficiency future devices.

REFERENCES

Born, M. and E. Wolf. 1999. Principles of Optics 7th Ed (Cambridge University Press) pp. 38–73.

Cavalcanti, S.B., M. de Dios-Leyva, E. Reyes-Gómez, and L.E. Oliveira. 2006. Band structure and band-gap control in photonic superlattices. Phys. Rev., B 74, 153102. doi: 10.1103/PhysRevB.74.153102.

DeSilva, L.A., R.G. Gadipalli, A. Donato, and T.M.W.J. Bandara. 2018. Reflectivity of 88% for four-period hybrid Bragg mirror from spin coating process. Optik, 157, 360–364. doi: 10.1016/j.ijleo.2017.11.048.

Dutta, H.S., A.K. Goyal, V. Srivastava, and S. Pal. 2016. Coupling light in photonic crystal waveguides: A review. Photonics Nanostructures: Fundam. Appl., 20, 41–58. doi: /10.1016/j.photonics.2016.04.001.

Hirose, K., Y. Liang, Y. Kurosaka, A. Watanabe, T. Sugiyama, and S. Noda. 2014. Watt-class high-power, high-beam-quality photonic-crystal lasers. Nature Photonics, 8, 406–411. doi: 10.1038/nphoton.2014.75.

Jewell, J.L., J.P. Harbision, A. Scherer, Y.H. Lee, and L.T. Florez. 1991. Vertical-cavity surface-emitting lasers - design, growth, fabrication, characterization. IEEE J. Quantum Electron, 27, 1332–1346. doi: 10.1109/3.89950.

Joannapoulos, J.D., S.G. Johnson, J.N. Winn, and R. Meade. 2008. Photonic Crystal, Modeling the Flow of Light (Princeton University Press) pp. 6–65.

John, S. 1987. Strong localization of photons in certain disordered dielectric superlattices. Phys. Rev Lett., 58, 2486. doi: 10.1103/PhysRevLett.58.2486.

Khreis, O.M. and A. Elhassan. 2013. A coupled-mode theory analysis of intermixing in semiconductor distributed Bragg reflectors. Opt. Quant. Electron., 45, 937–946. doi: /10.1007/s11082-013-9701-5.

Leem, J.W., X. Guan, and J.S. Yu. 2014. Tunable distributed Bragg reflectors with wide-angle and broadband high-reflectivity using nanoporous/dense titaniumdioxide film stacks for visible wavelength applications. Opt. Express, 28, 18519–18526. doi: /10.1364/OE.22.018519.

MATLAB (2020)stands for matric laboratory and it is a product developed by http://www.mathworks.com. A MATLAB clone exists, which is an open source package, available from www.gnu.org/software/octave/.

Noda, S., M. Fujita, and T. Asano. 2007. Spontaneous-emission control by photonic crystals and nanocavities. Nature Photonics, 1, 449–458. doi: 10.1038/nphoton.2007.141.

Schubert, M.F., J-Q. Xi, J.K. Kim, and E.F. Schubert. 2007. Distributed Bragg reflector consisting of high- and low-refractive-index thin film layers made of the same material. Appl. Phys. Lett., 90, 141115. doi: 10.1063/1.2720269.

Soman, A. and S.A. Antoney. 2018. Tuneable and spectrally selective broadband reflector – modulated photonic crystals and its application in solar cells. Solar Energy, 162, 525–532. doi: 10.1016/j.solener.2018.01.061.

Tkeshelashvili, L. 2013. Discrete optical soliton scattering by local inhomogeneities. Photonics Nanostruct: Fundam. Appl., 11, 95–101. doi: 10.1016/j.photonics.2012.10.001.

Yu, H-C., Z-W. Zheng, Y. Mei, R-B Xu, J-P. Liu, H. Yang, H, B-P. Zhang, et al. 2018. Progress and prospects of GaN-based VCSEL from near UV to green emission. Prog. Quant. Electron., 57, 1–19. doi: 10.1016/j.pquantelec.2018.02.001.

Zeng, L., P. Bermel, Y. Yi, B.A. Alamariu, K.A. Broderick, J. Liu, C. Hong, et al. 2008. Demonstration of enhanced absorption in thin film Si solar cells with textured photonic crystal back reflector. Appl. Phys. Lett., 93, 221105. doi: 10.1063/1.3039787.

APPENDIX

Below we give a simple MATLAB (2020) script that applies the theory to a Distributed Bragg Reflector.

```
%script begins here
%reflectivity_theory_applied.m
%Calculates the reflectivity versus wavelength for an Np period DBR
%by J. E. Hasbun and L. Ajith DeSilva
clear all;
clc;
th1=0.0;    %input incident angle in degrees (from the normal)
pif=pi/180;  %converting factor from degrees to radians
%Below, note sind is the sin(angle) function for angle in degrees
n1=1.0;     %incident index of refraction (air)
ns=1.5;     %substrate index of refraction
th1=th1*pif; %incident angle in radians
p1=n1*cos(th1);
%note: cos(ths)=sqrt(1-sin(ths)^2) and since ns*sin(ths)=n1*sin(th1)
%sin(ths)=n1*sin(th1)/ns
ps=ns*sqrt(1-(n1*sin(th1)/ns)^2);
%matrix elements associated with N periods. A period has two layers
%composed of indices n2 and n3
n2=1.63; %constant index of refraction of first layer
n3=2.72; %constant index of refraction of 2nd layer
h2=38;   %first layer thickness in nm
h3=50;   %second layer thickness in nm
Np=1;    %number of periods of interest
KF=2;    %interested in these Chebyshev polynomials here (pp 71, Born & Wolf)
      %KF=2 for Chebyshev polynomial (Second kind) Un(x) in function
      %ortho_poly.m (from www.mathworks.com/matlabcentral/fileexchange/)
Nwave_start=400; Nwave_end=1000;   %wavelength range in nm
Nwave_step=(Nwave_end-Nwave_start)/(Nwave_end-1);
for k=1:Nwave_end
```

```
  lambda(k)=Nwave_start+(k-1)*Nwave_step; %wavelength
  csth2=sqrt(1-(n1*sin(th1)/n2)^2);
  csth3=sqrt(1-(n1*sin(th1)/n3)^2);
  bet2=2*pi*n2*h2*csth2/lambda(k);
  bet3=2*pi*n3*h3*csth3/lambda(k);
  p2=n2*csth2;
  p3=n3*csth3;
  %transfer matrix for the first two layers
  %matrix for first layer is mb, and 2nd layer is mc
  %mb=[[cos(bet2),-1j*sin(bet2)/p2];[-1j*p2*sin(bet2),cos(bet2)]];
  %mc=[[cos(bet3),-1j*sin(bet3)/p3];[-1j*p3*sin(bet3),cos(bet3)]];
  %first period matrix is mbc and Np period matrix is mp
  %mbc=mb*mc; %one period transfer matrix
  mbc=[[cos(bet2)*cos(bet3)-p3*sin(bet2)*sin(bet3)/p2,...
       -1i*(cos(bet2)*sin(bet3)/p3+sin(bet2)*cos(bet3)/p2)];...
      [-1i*(p2*sin(bet2)*cos(bet3)+p3*cos(bet2)*sin(bet3)),...
       cos(bet2)*cos(bet3)-p2*sin(bet2)*sin(bet3)/p3]];
  %p=mbc^Np; %Np period transfer matrix
  %Chebyshev polynomials of KF kind, at x, of order NC: ortho_poly(KF,x,NC)
  ax=cos(bet2)*cos(bet3)-0.5*(p2/p3+p3/p2)*sin(bet2)*sin(bet3);
  unm1=ortho_poly(KF,ax,Np-1);
  if (Np-2 >= 0),
     unm2=ortho_poly(KF,ax,Np-2);
  else
     unm2=0;
  end
  %Np period transfer matrix using Chebyshev polynomials
  mp=[[mbc(1,1)*unm1-unm2,mbc(1,2)*unm1];[mbc(2,1)*unm1,mbc(2,2)*unm1-unm2]];
  %reflection (rn) and transmission (tn) coefficients
  deno=(mp(1,1)+mp(1,2)*ps)*p1+(mp(2,1)+mp(2,2)*ps);
  rn=((mp(1,1)+mp(1,2)*ps)*p1-(mp(2,1)+mp(2,2)*ps))/deno;
  tn=2*p1/deno;
  %reflectivity (R) and transmissivity (T)
  R(k)=abs(rn)^2;
%   T(k)=ps*abs(tn)^2/p1;
%   S(k)=R(k)+T(k);       %check unity
end
plot(lambda,R), xlabel('\lambda'), ylabel('R'), title('Reflectivity vs Wavelength')
axis([Nwave_start Nwave_end 0 max(R)*(1+0.1)])
%script ends here
```